ORIGINAL RESEARCH

Static and dynamic analysis of a non-homogenous embankment

Ali Moradi[1], Ehsan Delavari[2], Mohsen Saadat[3], Shamsa Basirat[4]

Abstract:

In this paper, for the first time, the vertical displacement of a non-homogenous embankment dam is investigated and evaluated in both static and dynamic states using FLAC software. In this regard, initially, the results obtained from this software are validated against the results of conventional methods. Subsequently, using FLAC software and 100 selected models, the impact of important dam parameters such as crest and core height on the vertical displacement of the dam is studied under various conditions in both static and dynamic states. The data analysis approach in this work involves considering a parameter as a witness. The witness parameter remains constant, and assuming that it does not participate in the analysis, one effective parameter and one criterion parameter are chosen for discussion and examination. For example, if the dam base is chosen as the witness parameter, and its value is intended to be 165 meters, the results have shown that an increase in the height of the earth dam leads to an increase in vertical displacements under static and dynamic loadings.

Keywords:
static analysis, dynamic analysis, FLAC, non-homogenous embankment dam

1. Introduction

Earth dams are significant structures that provide renewable energy and agricultural facilities. Due to their large size and capacity for storing substantial amounts of water, the safety and performance of dams are crucial considering environmental and economic considerations [1, 2]. When designing dam components, various factors and considerations must be carefully studied to ensure the quality and safety of the structure throughout its operational life. Earthquakes are among the most critical parameters to be evaluated during the design and operation of the structure. Given the possibility of earthquakes occurring during the structure's lifespan, minimizing potential damages by utilizing proper interaction between the structure and reservoir and selecting accurate parameters is essential. In this regard, dynamic and static analysis of the dam system is one of the most important aspects of design [3, 4]. A detailed study into the seismic behavior and stability of earth dams is an essential topic in geotechnical engineering and earthquake studies. Semi-static methods, block sliding methods, and numerical approaches are common techniques for estimating seismic deformations of earth dams [5]. In addition, many researchers have investigated the dynamic behavior of earth dams using numerical techniques [6-8]. These techniques allow for the examination of the behavior of geotechnical materials and structures under complex conditions and loading scenarios [9].
As mentioned, dynamic and static analysis of dams is one of the most critical factors for their safety. In this regard, researchers have conducted valuable research using various

✉*Corresponding author Email: e.delavari63@gmail.com
1 Department of civil engineering, Najafabad branch, Islamic Azad University, Najafabad, Iran
2 Department of civil engineering, Najafabad branch, Islamic Azad University, Najafabad, Iran
3 Department of civil engineering, Najafabad branch, Islamic Azad University, Najafabad, Iran

techniques. For example, Han et al. [10] investigated and simulated the seismic response of a concrete dam using the Coupled Hydro-Mechanical (HM) Dynamic Finite Element method. The study aimed to validate the numerical model for dynamic and static investigation of rock-fill dams against unique monitoring data recorded on the dam before and during the Wenchuan earthquake. The initial stress state for dynamic analysis was simulated by reproducing the geological history of the dam foundation, dam construction, and reservoir impoundment. Subsequently, the predicted seismic response of the dam in terms of deformation, crown settlements, and acceleration distribution patterns was investigated to understand seismic behavior, study its seismic safety, and provide indications for potential reinforcement measures. Dong and Yu [11] focused on the numerical dynamic and static analysis of an embankment dam. The three-dimensional static analysis of the dam with a tall core was performed using the Duncan-Chang E-B model. The dynamic study of the dam under earthquake using the EB3D program employed both traditional viscoelastic modeling and linear equivalent modeling based on the initial static stress. The dynamic response of the dam throughout the earthquake process was investigated using the FEMEPDYN program, which is based on the elastoplastic model and nonlinear analysis technique. The dynamic behavior of the embankment dam during the earthquake was studied, and seismic response characteristics were investigated. The outcomes showed that the predicted seismic deformation of the embankment dam aligns with field observations, demonstrating the dam's safe performance during the Wenchuan earthquake. Zewdu [12] studied the stability and analysis of an embankment dam using PLAXIS 2D finite element software. The behavior of the embankment dam body and foundation was described using the Mohr-Coulomb criterion. The safety factors at the end of construction for dynamic and static stability analysis were 1.6221 and 1.3592, respectively. For the stable condition, the reservoir water level was fixed at the normal level (2015.25 meters), yielding safety factors of 1.6136 and 1.3157 for dynamic and static analyses, respectively. The study results indicated a decrease in the discharge conditions from a normal reservoir level of 2015.25 meters to 2008.5 meters. Furthermore, the safety factors for static and dynamic analyses were 1.2199 and 1.0353, respectively. The displacement results indicate that the maximum total displacement for static and dynamic analysis are 1.33% and 1.628% of the dam height, respectively. These results have been validated with the benchmarks presented in reference [13]. Chebout and Bahar [14] conducted the numerical analysis using the finite difference method to study the static and dynamic behavior of an embankment dam in Africa. The study considered material behavior, soil-structure interaction, dam behavior during hydraulic conditions, and saturation effects. The dynamic and study analysis of a soil dam named Codara, located in the Boumerdes region (Algeria), was conducted using the finite difference method (FLAC 3D). The aim was to determine its behavior in terms of settlement and deformation. Pressure changes in the pores during construction and operation were intended in two stages in this study. Two mathematical techniques, elastic and Mohr-Coulomb models, were employed for static analysis to examine the dam in two stages: dam construction and water filling. For dynamic analysis, both elastic and Mohr-Coulomb models were employed to perform a coupled dynamic analysis with actual earthquake records, considering the interaction between the fluid and solid phases.

The examination of past research shows that, until now, dynamic and static analysis of non-homogenous embankment dams using the FLAC software has not been performed. Based on this background, this paper will, for the first time, delve into the static and dynamic analysis of an embankment dam using the FLAC software. In this regard, the initial step involves validating the results obtained from the FLAC software against the outcomes of other methods. Subsequently, the impact of critical dam parameters on the vertical

displacement of the dam in both static and dynamic states will be studied and evaluated.

2. Static and dynamic analysis of the dam using FLAC

The As stated, the objective of this paper is to investigate an embankment dam from both static and dynamic perspectives using the FLAC software. These analyses were conducted for 100 different models with varying geometric parameters. To control decision parameters and select the optimal function, the outputs of static and dynamic analyses using the FLAC software were studied. Before investigating the static and dynamic displacement of the dam for each change in design parameters, it is necessary to validate the chosen technique (i.e., the use of FLAC).

It is noteworthy that the dynamic analysis of the earth dam has been conducted under an earthquake-like load. In this context, the excitation is applied as a known signal with specified displacement, velocity, and acceleration. Fig. 1 depicts the intended excitation. As can be seen in Fig. 1, the maximum recorded acceleration for this signal is 48.8 cm/s^2. The peak velocity is 1.96 cm/s^2, and the peak displacement is 1.23 mm. The acceleration spectrum is shown in Fig. 1. According to Fig. 2, the dominant frequencies of this signal happen between 2 and 12 Hz.

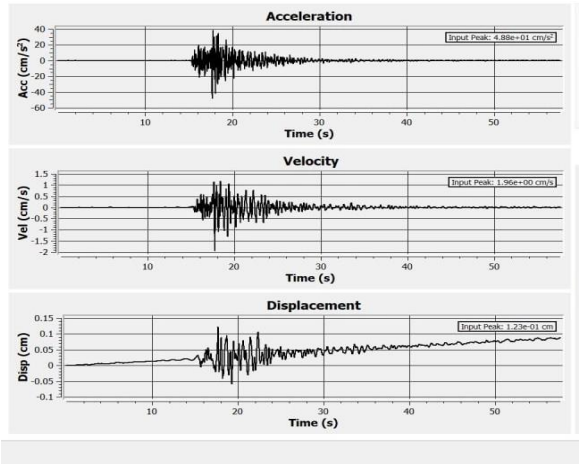

Fig. 1. Excitation input to the problem in the form of an earthquake signal.

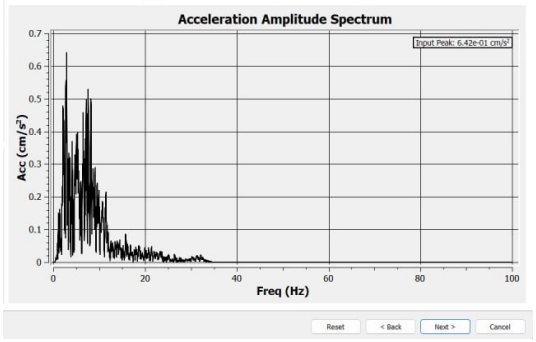

Fig.2. the spectrum of the excitation acceleration size.

Also, Fig. 3 shows the main geometry of the model. Also, the specifications of the model are explained in Table 1.

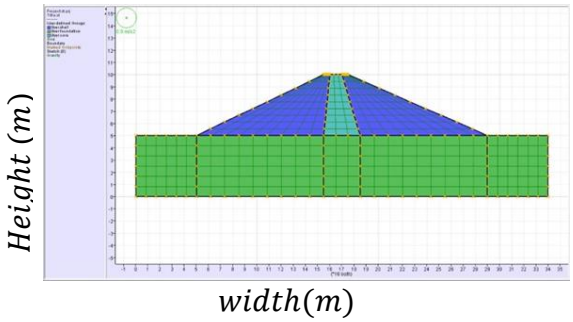

Figure. 3 the model used in the FLAC software.

Table 1- Properties of the foundation and core of the embankment dam and shell used as input data in the simulation.

Properties	Units	foundation	core of the embankment dam	shell
Dry density	kg/m^3	2200	1800	2000
Young's modulus	MPa	1000	40	60
Poisson's rate		0.25	0.3	0.3
Shear stress module	MPa	400	15.38	23.08
Bulk module	MPa	666.67	33.33	50
stickiness	kPa	-	100	0.1
Angle of plastic friction	Degree	-	15	35
Dilation Angle	Degree	-	3	10

With the use of a "fully automatic" meshing scheme and the available default settings, there

was no need to draw individual finite elements. A default mesh was created after the geometric regions were defined. However, the generated default mesh can be modified globally or locally as needed. Each finite element contains "nodes" that are used to describe how the initial unknown parameters are distributed within the element, thus contributing to the development of finite elements. In finite element formulation, it is necessary to adopt a model that describes the linear or nonlinear distribution of the primary variable within the element (e.g., the total head of a dam). For a linear distribution of the initial unknown, nodes are only required at the corners of the element. With three or more nodes defined along the edge of an element, a quadratic or any higher-degree equation can be used to describe the distribution of the initial unknown. Compatibility between different elements is established through their shared nodes, ensuring the common distribution of initial unknown parameters along the shared edge of the elements. A special integer-based algorithm is also used in FLAC to check for consistency between regions. The robustness of the meshing algorithm affects the number of divisions along the edge of a region and may actually be higher than what is specified as "default." Different finite element mesh patterns are available as defaults in FLAC, namely (a) quadrilateral and triangular, (b) triangular only, (c) rectangular quadrilateral mesh, and (d) quadrilateral/triangular triangular mesh. In general, the element size (e.g., 0.5) is used for main regions, while the adjusted element size (expressed as the "default size ratio") is used along the intersections of different regions with different components. The total number of nodes and elements used in the finite element model depends on the number of mesh elements used and the adjustments adopted. In the present study, the model domain was discretized into an unstructured grid consisting of first-order quadrilateral and triangular elements. Based on the geometry and adopted adjustments, the domain includes 1,636 nodes and 1,531 elements. The overall element size used for the base model is 1 meter, while local refinements resulted in mesh elements with a size of 0.3 meters, minimizing it to that extent.

The boundaries at the left and right ends of this numerical model are restricted to displacements in the horizontal direction (Cartesian coordinate x), while the bottom edge is constrained to displacements in both the horizontal and vertical directions (Cartesian coordinates x and y). Similarly, the appropriate boundary conditions for displacement are applied to the domain boundaries. Sections of the domain boundaries that need to remain free and exhibit displacement are not "fixed" in any direction. Additionally, to simulate the water pressure from the reservoir, a fluid pressure boundary is defined on the upstream surface of the dam by specifying the water level. The software used applies both types of boundary conditions—fixed pressure and variable pressure boundaries—to represent the constant and fluctuating reservoir levels, respectively, under steady-state and variable reservoir conditions.

In this study, boundary conditions play a crucial role in the final seismic responses of the numerical dam model. To examine this impact, two different stages of boundary conditions were applied to the numerical model. In the first stage, which includes the pre-analysis phase, static loading was applied to the model by imposing water pressure exceeding the usual level in the reservoir on the upstream side of the numerical model. During this stage, the sides of the numerical model were considered fixed. Additionally, a "fixed" type of support was employed. Specific boundary conditions were also applied to the base of the model in both directions of the two-dimensional plane of modeling.

In the second stage, which includes the dynamic analysis phase, the desired earthquake acceleration was applied to the bedrock of the numerical model. To prevent the negative effects of seismic waves at the boundaries and to avoid their reflection back into the numerical model, leading to errors, dynamic boundaries were defined using absorbing boundaries with viscous dampers. In this method, dampers are used at the model boundaries instead of the usual static fixations.

Through these dampers, stresses on the model boundaries are absorbed, preventing the generation of errors.

The materials of the earth dam and foundation are modeled using an "elastic-plastic" material model for stress-deformation analysis. In this analysis, the materials of the earth dam are modeled using a saturated/unsaturated material model, while the foundation is modeled using a "saturated" material model. The water content function and hydraulic conductivity function are used as inputs for the materials selected for the earth dam and foundation.

Additionally, the hydraulic head at each node is essentially unknown and is related to the hydraulic head (H) and the flow values (Q) that are predefined or specified at certain nodes in the domain. Specific values of H or Q are applied as boundary conditions. In steady-state analysis, at least one node in the entire mesh must be assigned a specified value of H. Various boundary conditions such as head (H), total flux (Q), unit flux (q), unit gradient (i), and pressure head (P) are required to be applied. In this study, a constant total head boundary condition or a head boundary condition accounting for temporal variations is considered to determine steady-state conditions and reservoir level fluctuations, respectively. At the upstream end of the surface, the reservoir capacity level is considered to be about 25 meters, and accordingly, a total head boundary condition of 25 meters is applied. On the downstream side of the dam, the groundwater level is considered to be at ground level. The ground elevation at the bottom of the reservoir is 10 meters, so an H = 10 meter boundary condition is applied at the downstream end. Along the downstream surface of the dam, a potential seepage face is also marked as a boundary condition with zero flux (Q = 0), indicating that no additional flux is added or removed at these nodes. This boundary condition ensures that if the phreatic surface or any flow line intersects the slope, there will be no accumulation of water on the downstream surface.

The ground elevation at the reservoir surface is 10 meters, and accordingly, a head of 10 meters is applied in the downstream flow. Along the downstream surface of the dam, a potential orifice face is also marked as a boundary condition with zero flux (Q = 0), indicating that no additional flux is added or removed at these nodes. This boundary condition ensures that there is no water accumulation on the downstream flow surface where the phreatic surface or any flow lines intersect with the flow slopes. Moreover, various boundary conditions are implemented to account for different deformation scenarios during modeling. Essentially, there are only two types of boundary conditions that can be applied for stress-deformation analysis: "stress" and "force or displacement" boundary conditions. In the "stress type" category, hydrostatic pressure boundary conditions (whether the fluid height is constant or varying with time) are used to simulate the conditions of a stable or fluctuating reservoir, respectively.

In summary, it can be stated that in all stress-deformation models, defining a boundary for the problem is crucial, meaning that certain parts of the geometry must be defined as "zero displacement" boundary conditions. Typically, the far left and right boundaries of a numerical model are restricted to horizontal displacement (x-axis), while displacement at the bottom edge is restricted in both horizontal and vertical directions (x and y axes). Accordingly, appropriate zero displacement boundary conditions were applied to the domain boundaries. Additionally, to simulate the reservoir water pressure, a fluid pressure boundary condition was defined on the upstream face of the dam by specifying the water level.

2.1.Validation

To validate the modeling and ensure the accuracy of the results obtained from FLAC software, some of the outcomes in this study have been compared with previous studies. The study chosen for this purpose is the study by Talukdar and Dey [15]. In this mentioned study, finite element analysis is employed for the analysis of the structure under consideration. Figure 4 shows a sample of the geometry and domain meshing for

computational calculations. Figure 4c represents the same model as the article in the FLAC software, which is used for validating the modeling. With a rule of 100 and a crown width of 4 meters, this model is considered suitable for validation due to its proximity to the average dimensions selected for optimization.

The intended model includes two different conditions for the dam crest. As seen in Figure 4, the upper part of the dam is constructed in both single-stage and multi-stage configurations. The difference in these two lift conditions for the crest is observed in ref [15]. Some of the results presented in [15] also highlight the distinction between these two lift conditions of the structure.

The model shown in Figure 4, presented for the validation of the software results, has been appropriately categorized. The side sections of the dam base, due to the least strain created, are well separated from the center of the base. In addition, the core and crest sections are considered separate components due to their high significance in analysis and modeling. It is possible to study them separately.

Also, Fig. 5 shows the different parts of the structure of the model. This division of the network is done for faster and easier access to the examined sections. For this purpose, the clay core part of the dam is separated from the other parts. In the crown of the dam, the grid has been done more finely.

Figure 5 illustrates the horizontal displacement of the structure under loading. The upper part represents a uniform lift condition, while the lower part represents a multi-stage lift condition. As shown, in the case of a uniform lift, the maximum displacement of the structure is four times greater than the multi-stage lift condition, as also described in reference [15]. In the uniform lift condition, the maximum displacement is 0.04 meters, whereas in the multi-stage lift condition, it is approximately 0.01 meters.

The maximum displacement in the current work is almost equal to the maximum horizontal displacement obtained in the study [15], indicating the correctness of the modeling trend. More results related to this comparison can be observed in Table 2. As seen in Table 2, the range of variation in the results of this work is entirely consistent with the results obtained in reference [15]. Therefore, it can be confidently understood that the current modeling is entirely accurate, and the results are reliable. Accordingly, with full confidence, modeling with more parameters can be performed on this type of earth dam, and the outcomes obtained can be used for database creation and, consequently, optimization.

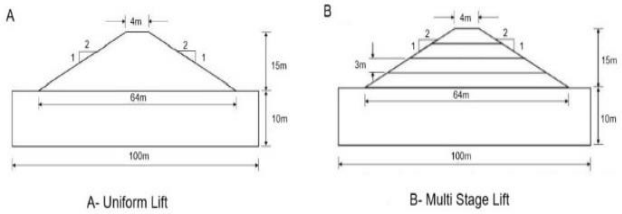

Figure. 4 – Geometry and domain meshing in the reference [15]

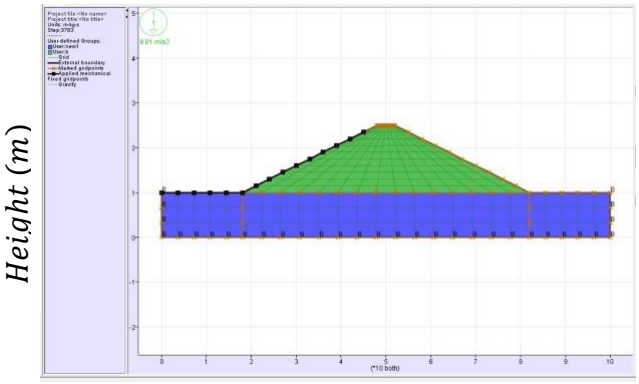

Fig. 5. the model used for validating the results in the FLAC software

Table 2: Comparison of the Results of the Present Study with the Ref [15]

Parameter	Ref [15]	This study
The maximum displacement at the top of the dam (m)	0.03 to 0.04	**0.03**
The maximum displacement at the bottom of the dam (m)	0.03 to 0.04	**0.03**
The maximum displacement in the structure (m)	0.05	**0.03**

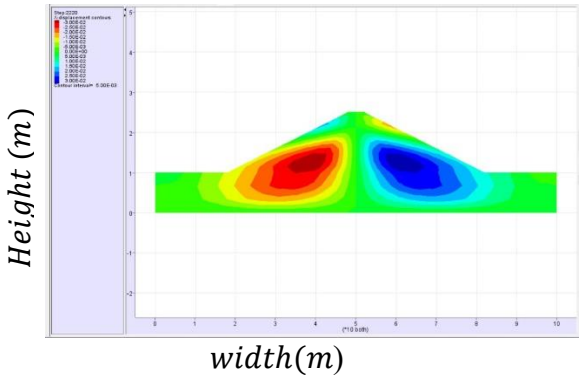

Fig. 6: Horizontal displacement distribution obtained from the present study.

In the previous section, the validation of the method used to examine the vertical displacement of the dam in two static and dynamic states was discussed. In this section, the main goal of the paper, which is to study the influence of each of the important parameters of the dam on the two mentioned factors, will be investigated and analyzed.

The approach to data analysis in this study is such that one parameter is considered as a witness. This witness parameter remains constant, and assuming it does not participate in the analysis, an effective parameter and two criterion parameters for discussion and examination will be selected. For example, in Table 3, a sample of such selection is provided. In this example, the dam base is considered as the witness parameter. The core base is the effective parameter, and the first and second criterion parameters are static and dynamic displacements of the structure, respectively.

Table 3. An example of selection witness, effective and criterion parameters for data analysis

Criterion parameter value 2	Criterion parameter value 1	Effective parameter	Witness parameter	Model number
-0.25	-0.3	40	150	**4**
-0.3	-0.3	50	150	**30**
-0.3	-0.3	50	150	**31**
-0.3	-0.3	40	150	**32**
-0.2	-0.2	40	150	**33**
-0.24	-0.225	40	150	**34**
-0.22	-0.225	30	150	**35**
-0.19	-0.175	22	150	**75**
-0.19	-0.175	22	150	**76**
-0.22	-0.225	22	150	**77**
-0.22	-0.225	22	150	**78**
-0.22	-0.225	22	150	**79**

Figure 8 shows the static and dynamic displacements of the structure for all 100 models examined in this study. As observed, the minimum simultaneous dynamic and static displacements are associated with models 75, 76, and 83. The maximum vertical displacement recorded corresponds to model number 1.

In the case of selecting a sample according to Table 3, the vertical static and dynamic displacements can be well examined as shown in Figure 9. In this case, the dam base is fixed at 150. In general, with all parameters being constant, they will not have any effect on the comparisons, allowing for an easy comparison of different models in terms of effective and criterion parameters. It is observed that an increase in the core base leads to an increase in both static and dynamic displacements. For example, increasing the base from 22 meters to 50 meters results in almost a 1.5-fold increase in static and dynamic displacements. The effect of the dam crest is shown in Figure 10. It is visible that under these conditions, changes in the dam crest have a much smaller effect on dynamic and static displacements compared to the core base. Figure 11 shows the effect of dam height on static and dynamic displacements. In this example, the dam base is selected as the witness parameter with a length of 150 meters. It is observed that the changes in dam height have a significant effect on vertical displacements. Figure 12 illustrates the effect of the core crest on static and dynamic displacements. As shown in Figure 12, changes in the core crest have relatively little effect on displacements.

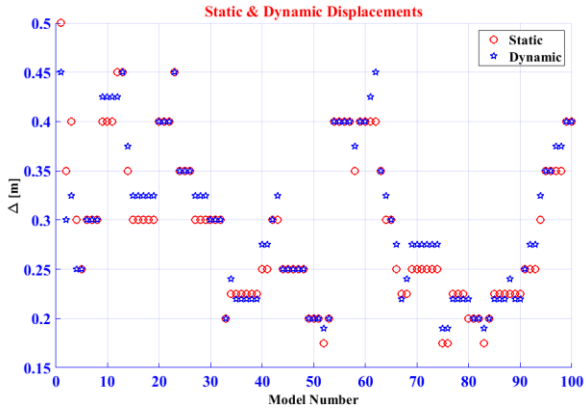

Figure 7. Static and dynamic displacements of all 100 models under investigation.

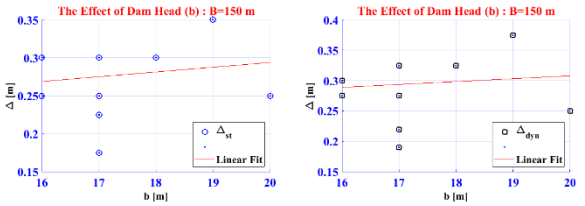

Figure 8. The effect of the clay core base on static and dynamic vertical displacements**.**

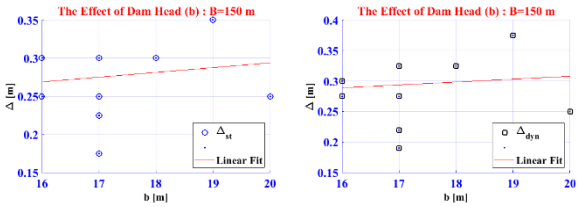

Figure 9. The effect of the dam crest on static and dynamic vertical displacements

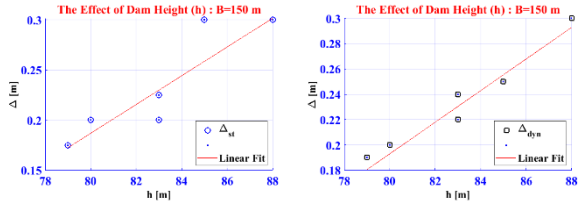

Figure 10. The effect of the dam height on static and dynamic vertical displacements

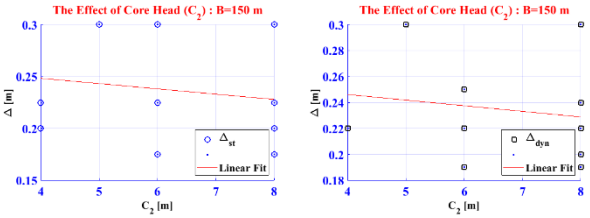

Figure 11. The effect of the core crest on static and dynamic vertical displacements.

Continuing, in another example, the crest width of the dam is considered as the witness parameter. In this example, the crest width is fixed and equal to 15 meters. Figure 13 depicts the effect of the core base on static and dynamic displacements. A noticeable increase in both dynamic and static displacements is observed with an increase in the core base. The effect of height is shown in Figure 14. An increase in height clearly leads to an increase in static and dynamic displacements. Additionally, Figure 15 demonstrates the effect of the dam base on displacements. A 1.5-fold increase in static and dynamic displacements is observed with an increase in the dam base. The values for this example are available in Table 4.

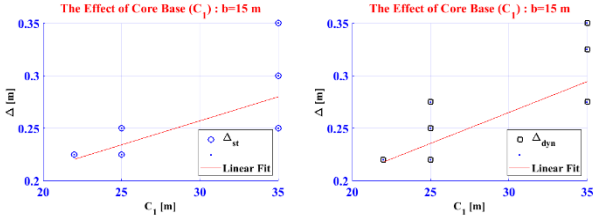

Figure 12. The effect of the core base on static and dynamic vertical displacements.

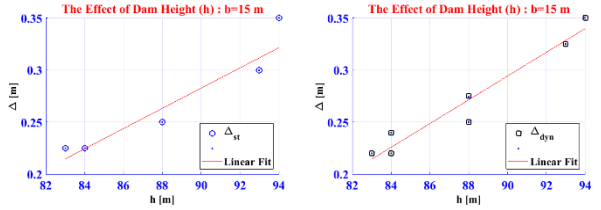

Figure 13. The effect of the dam height on static and dynamic vertical displacements.

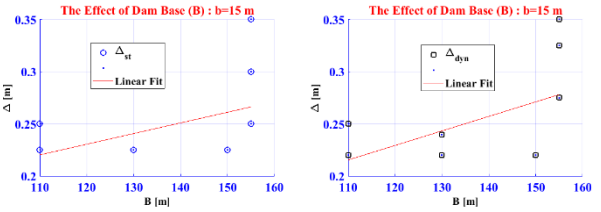

Figure 14. The effect of the dam base on static and dynamic vertical displacements.

Table 4. An example comprising the crest width (b) as the controlling parameter and the dam base (B) as the influential parameter.

Criterion parameter value 2	Criterion parameter value 1	Effective parameter	Witness parameter	Model number
-0.22	-0.225	110	15	**90**
-0.25	-0.25	110	15	**91**
-0.22	-0.225	130	15	**89**
-0.22	-0.225	130	15	**87**
-0.24	-0.225	130	15	**88**
-0.22	-0.225	150	15	**78**
-0.22	-0.225	150	15	**79**
-0.275	-0.25	155	15	**92**
-0.275	-0.25	155	15	**93**
-0.325	-0.3	155	15	**94**
-0.35	-0.35	155	15	**95**

If the dam base is chosen as the witness parameter with a value of 165 meters, and once again the effect of dam height is examined as the effective parameter, a noticeable increase in static and dynamic displacements is still observed. Figure 16 shows the effect of dam height on static and dynamic displacements. It is evident that an increase in dam height leads

to an increase in vertical displacements under both static and dynamic loadings. This is not surprising, as an increase in height results in a longer span under load.

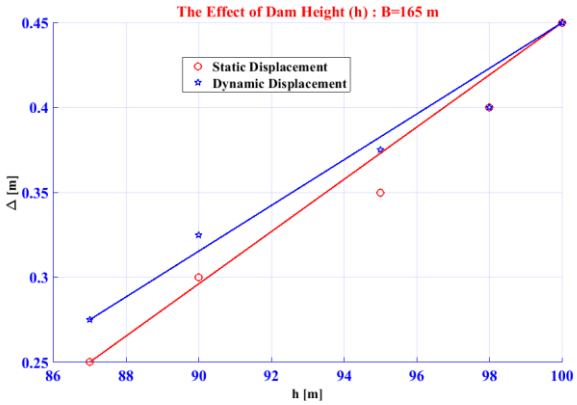

Figure 15. The effect of increasing dam height on static and dynamic displacements.

If the core crest width is chosen as the witness parameter, and the effect of other geometric parameters is examined, it will still be observed that an increase in dam height leads to an increase in static and dynamic displacements. Figure 17 also illustrates the effect of the core base on dynamic and static displacements with the core crest width as the witness parameter. An increase in displacement is clearly visible in this case for an increase in either the core base or the dam height. These changes are also well observable in Table 5. Figure (18) illustrates the effect of dam height on static and dynamic displacements with a core crest width of 7 meters. Also, in Figures 19 and 20, the respective effects of the dam base and the dam crest on static and dynamic displacements are shown. The results show that the dam crest alone does not have a significant effect on displacements, and this parameter should be considered in combination with other geometric parameters to observe its impact. However, the dam base has a clear and significant effect on both static and dynamic displacements.

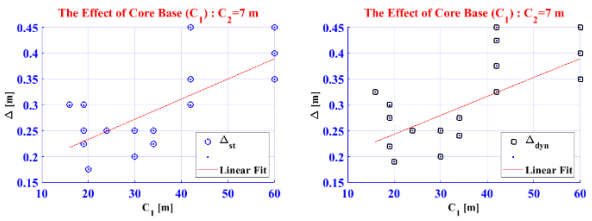

Figure 16. The effect of the core base on static and dynamic displacements.

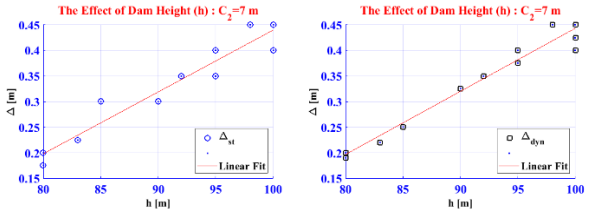

Figure 17. The effect of dam height on static and dynamic displacements

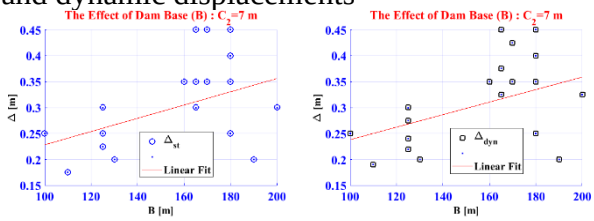

Figure 18. The effect of dam base on static and dynamic displacements

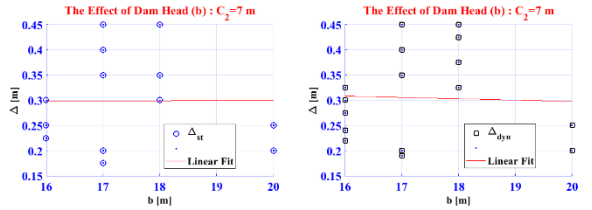

Figure 19. The effect of the dam crest on static and dynamic displacements.

Table 5. An example comprising the core crest width (C2) as the controlling parameter and the dam base (B) and dam height (h) as the influential parameters**.**

Criterion parameter value 2	Criterion parameter value 1	Effective parameter 2	Effective parameter 1	Model number
-0.25	-0.25	90	100	**5**
-0.19	-0.175	80	110	**52**
-0.22	-0.225	84	125	**67**
-0.275	-0.25	89	125	**66**
-0.3	-0.3	92	125	**65**
-0.24	-0.225	84	125	**68**
-0.275	-0.25	87	125	**69**
-0.2	-0.2	80	130	**51**
-0.35	-0.35	92	160	**26**
-0.325	-0.3	90	165	**15**
-0.375	-0.35	95	165	**14**
-0.45	-0.45	100	165	**13**

-0.425	-0.45	100	170	**12**
-0.35	-0.35	92	170	**25**
-0.25	-0.25	85	180	**48**
-0.35	-0.35	92	180	**24**
-0.4	-0.4	95	180	**22**
-0.45	-0.45	98	180	**23**
-0.2	-0.2	80	190	**50**
-0.2	-0.2	80	190	**49**
-0.325	-0.3	93	200	**64**

Analysis of the results obtained from the optimization process shows that if the dam height is chosen as the witness parameter and the effect of the dam crest on dynamic and static displacements is examined, it becomes apparent that with an increase in the dam crest, both static and dynamic displacements will decrease (Figure 21). Although this reduction is around 25%, it indicates that examining the effect of a parameter in isolation may not be sufficient, and its impact should be considered in different combinations.

Still, in Figure (22), it can be observed that an increase in the dam base leads to an increase in displacements. Figure (23) also illustrates the effect of the core base on displacements. The results show the minimal effect of this parameter on displacements, given the constant height.

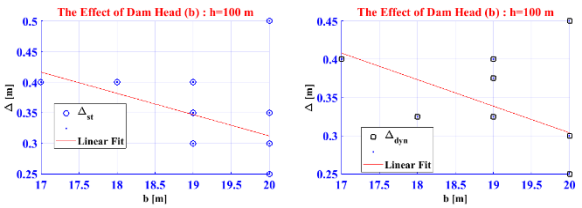

Figure 20. The effect of the dam crest on static and dynamic displacements.

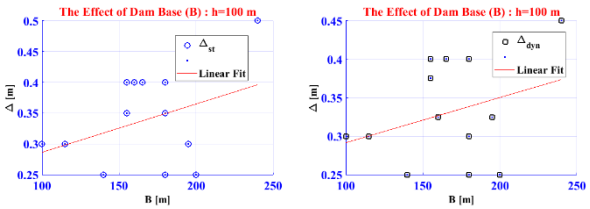

Figure 21. The effect of the dam base on static and dynamic displacements**.**

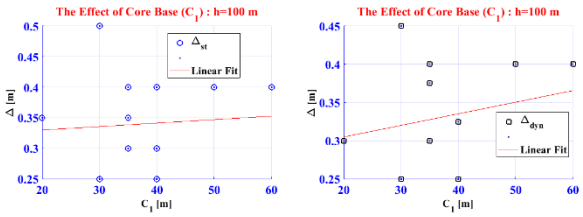

Figure 22. The effect of the core base on static and dynamic displacements.

In another example, the core base is considered as the witness parameter. In this case, the effect of four other geometric parameters was examined, showing that an increase in the core crest leads to a 25% reduction in static and dynamic displacements (Figure 24). Additionally, the results indicate that an increase in height and dam base leads to an increase and decrease in static and dynamic displacements, respectively (Figures 25 and 26). However, in Figure 27, it is observed that an increase in the dam crest has not much effect on static and dynamic displacements.

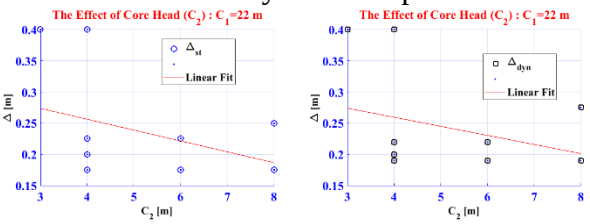

Figure 23. The effect of the core crest on static and dynamic displacements.

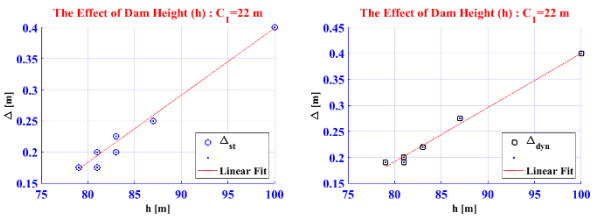

Figure 24. The effect of dam height on static and dynamic displacements.

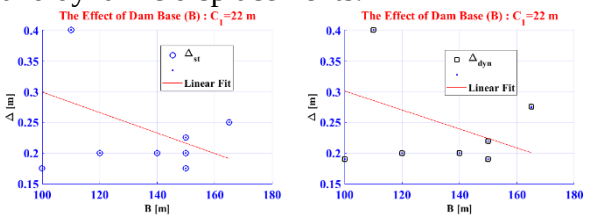

Figure 25. The effect of dam base on static and dynamic displacements.

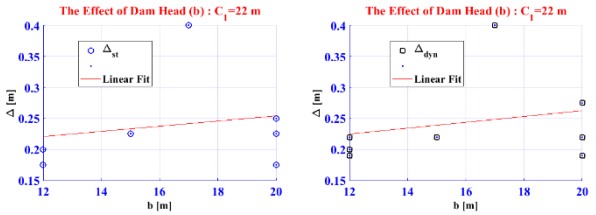

Figure 26. The effect of the dam crest on static and dynamic displacements.

3. conclusion

In In this article, for the first time, the vertical displacement in both static and dynamic states of a non-homogenous embankment dam was examined and evaluated using FLAC software (for 100 models). In this regard, the simulations conducted with FLAC software were validated against the results of a reputable article. The approach to data analysis in this study was to consider one parameter as a reference. This witness parameter remained constant, and assuming it did not participate in the analysis, an effective parameter and a criterion parameter were selected for discussion and examination. The most important results related to this study are presented in MATLAB as follows:

1) It was observed that the minimum simultaneous dynamic and static displacement is related to models 75, 76, and 83, and the maximum vertical displacement recorded is associated with model number 1.

2) It was observed that an increase in the base of the earth dam leads to an increase in both static and dynamic displacements. For example, an increase in the base from 22 meters to 50 meters results in nearly a twofold increase in static and dynamic displacements.

3) In one sample, the base of the dam was selected as the witness parameter with a length of 130 meters. It was observed that the changes made in the dam crest have minimal impact on vertical displacements. In fact, the range of variations in displacements is very small, and the effect of the dam crest can be overlooked.

4) In another sample, the effect of the base of the dam on static and dynamic displacements was illustrated. In this sample, the crest width was kept constant at 15 meters. A noticeable increase in dynamic and static displacements was observed with an increase in the dam base.

5) If the base of the dam is chosen as the witness parameter, with a value of 165 meters, the effect of the dam height as the influential parameter can be investigated. In one case, the impact of the dam height on static and dynamic displacements was examined. It was clearly observed that an increase in the height of the earth dam leads to an increase in vertical displacements under both static and dynamic loading.

6) In two samples, the crest width was considered as the witness parameter, and its value was set to a constant 7 meters. In this scenario, the effect of two different geometric parameters on vertical static and dynamic displacements was investigated. The analyses indicated that an increase in the dam height, as well as the base of the dam, results in an increase in both dynamic and static displacements.

The use of MATLAB for optimizing the problem and investigating the impact of various geometric parameters has resulted in the creation of a highly useful database in this study. This database can also be leveraged for other purposes.

4. References

1. Raja, M.A. and B.K. Maheshwari, *Behaviour of earth dam under seismic load considering nonlinearity of the soil.* Open Journal of Civil Engineering, 2016. **6**(02): p. 75.
2. Elia, G., et al., *Fully coupled dynamic analysis of an earth dam.* Géotechnique, 2011. **61**(7): p. 549-563.
3. Naylor, D., *Constitutive laws for static analysis of embankment dams*, in *Applications of Computational Mechanics in Geotechnical Engineering*. 2021, Routledge. p. 289-316.
4. Sharafi, A., *Static analysis of soral embankment dam during operation using precise dam tool data and finite element method.* Journal of Critical Reviews, 2020. **19**(7): p. 9089-9101.
5. Meehan, C.L. and F. Vahedifard, *Evaluation of simplified methods for predicting earthquake-induced slope displacements in earth dams and embankments.* Engineering Geology, 2013. **152**(1): p. 180-193.
6. Gordan, B., et al., *Review on dynamic behaviour of earth dam and embankment during an earthquake.* Geotechnical and Geological Engineering, 2022. **40**(1): p. 3-33.
7. Lyapichev, Y.P., *Choice of mathematic models of soils in static and seismic analyses of embankment dams.* Structural mechanics of engineering constructions and buildings, 2020. **16**(4): p. 261-270.
8. Khan, M. and M. Seyedi, *Dynamic responses of embankment dams, constituted from varied soil types, to seismic activity.* Acadlore Trans. Geosci, 2023. **2**(3): p. 177-187.
9. Prasad, K., et al., *A variably saturated numerical model for seepage and stability analyses of an embankment dam with a central core.* International Journal of Geotechnical Engineering, 2010. **4**(1): p. 139-150.
10. Han, B., et al., *Numerical investigation of the response of the Yele rockfill dam during the 2008 Wenchuan earthquake.* Soil Dynamics and Earthquake Engineering, 2016. **88**: p. 124-142.
11. Dong, W. and Y. Yu. *Static and dynamic analyses of high core rockfill dams*. in *Constitutive Modeling of Geomaterials: Advances and New Applications*. 2013. Springer.
12. Zewdu, A., *Modeling the slope of embankment dam during static and dynamic stability analysis: a case study of Koga dam, Ethiopia.* Modeling Earth Systems and Environment, 2020. **6**(4): p. 1963-1979.
13. Fell, R., et al., *Time for development of internal erosion and piping in embankment dams.* Journal of geotechnical and geoenvironmental engineering, 2003. **129**(4): p. 307-314.
14. Chebout, S. and R. Bahar, *Static and Dynamic Analysis of Keddara Dam.* International Journal of Engineering Research in Africa, 2022. **62**: p. 71-84.
15. Talukdar, P. and A. Dey, *Finite element analysis for identifying locations of cracking and hydraulic fracturing in homogeneous earthen dams.* International Journal of Geo-Engineering, 2021. **12**: p. 1-26.